

This discussion paper is/has been under review for the journal Atmospheric Chemistry and Physics (ACP). Please refer to the corresponding final paper in ACP if available.

# Beyond direct radiative forcing: the case for characterizing the direct radiative effect of aerosols

C. L. Heald<sup>1,2</sup>, D. A. Ridley<sup>1</sup>, J. H. Kroll<sup>1</sup>, S. R. H. Barrett<sup>3</sup>, K. E. Cady-Pereira<sup>4</sup>, M. J. Alvarado<sup>4</sup>, and C. D. Holmes<sup>5</sup>

<sup>1</sup>Department of Civil and Environmental Engineering, Massachusetts Institute of Technology, Cambridge, MA, USA

<sup>2</sup>Department of Earth, Atmospheric and Planetary Sciences, Massachusetts Institute of Technology, Cambridge, MA, USA

<sup>3</sup>Department of Aeronautics and Astronautics, Massachusetts Institute of Technology, Cambridge, MA, USA

<sup>4</sup>Atmospheric and Environmental Research (AER), Lexington, MA, USA

<sup>5</sup>Department of Earth System Science, University of California, Irvine, CA, USA

Received: 14 November 2013 – Accepted: 4 December 2013 – Published: 16 December 2013

Correspondence to: C. L. Heald (heald@mit.edu)

Published by Copernicus Publications on behalf of the European Geosciences Union.

ACPD

13, 32925–32961, 2013

Discussion Paper | Discussion Paper

## Beyond direct radiative forcing

C. L. Heald et al.

[Title Page](#)

[Abstract](#)

[Introduction](#)

[Conclusions](#)

[References](#)

[Tables](#)

[Figures](#)

[|◀](#)

[▶|](#)

[◀](#)

[▶](#)

[Back](#)

[Close](#)

[Full Screen / Esc](#)

[Printer-friendly Version](#)

[Interactive Discussion](#)



## Abstract

ACPD  
13, 32925–32961, 2013

The direct radiative effect (DRE) of aerosols, which is the instantaneous radiative impact of all atmospheric particles on the Earth's energy balance, is often confused with the direct radiative forcing (DRF), which is the change in DRE from pre-industrial to present-day (not including climate feedbacks). We use here a coupled global chemical transport model (GEOS-Chem) and radiative transfer model (RRTMG) to contrast these concepts. We estimate a global mean all-sky aerosol DRF of  $-0.36 \text{ Wm}^{-2}$  and a DRE of  $-1.83 \text{ Wm}^{-2}$  for 2010. Therefore, natural sources of aerosol (here including fire) affect the global energy balance over four times more than do present-day anthropogenic aerosols. If global anthropogenic emissions of aerosols and their precursors continue to decline as projected in recent scenarios due to effective pollution emission controls, the DRF will shrink ( $-0.22 \text{ Wm}^{-2}$  for 2100), while the climate feedbacks on aerosols under rising global temperatures will likely amplify. Secondary metrics, like DRE, that quantify temporal changes in both natural and anthropogenic aerosol burdens are therefore needed to quantify the total effect of aerosols on climate.

## 1 Introduction

Atmospheric aerosols are the most uncertain driver of global climate change (IPCC, 2013). These particles can scatter or absorb radiation, thereby cooling or warming the Earth and its atmosphere directly. They also play a pivotal role in cloud formation, acting as nuclei for liquid or ice water clouds, and can thus indirectly cool the planet by increasing its albedo. The overall impact of present-day atmospheric aerosols is estimated to be a cooling, globally counterbalancing a significant fraction of the warming associated with greenhouse gases (IPCC, 2013). There is thus a critical need to better quantify the role of aerosols in the climate system. The ability of aerosols to modify climate depends on their atmospheric abundance over time as well as their chemical,

## Beyond direct radiative forcing

C. L. Heald et al.

[Title Page](#)

[Abstract](#)

[Introduction](#)

[Conclusions](#)

[References](#)

[Tables](#)

[Figures](#)

[◀](#)

[▶](#)

[Back](#)

[Close](#)

[Full Screen / Esc](#)

[Printer-friendly Version](#)

[Interactive Discussion](#)



physical, and optical properties; uncertainties on all of which are large (Myhre et al., 2013; Kinne et al., 2006).

The direct radiative effect (DRE) is Earth's instantaneous radiative flux imbalance between incoming net solar radiation and outgoing infrared radiation resulting from the presence of a constituent of the Earth's atmosphere. This is distinct from direct radiative forcing (DRF), a leading climate-relevant metric for aerosol (and other constituents), commonly used to quantify aerosol impacts (e.g. Shindell et al., 2009) and in international assessment (e.g. IPCC, 2013). Generally, DRF quantifies the change in DRE over time which will induce a change in global temperatures. In the context of the IPCC climate assessments, this time horizon has been specified as pre-industrial to present-day (IPCC, 1990, 1995, 2001, 2007, 2013). In this IPCC framework, the radiative forcing has also been restricted to "denote an externally imposed perturbation" (IPCC, 2001), and so excludes feedbacks resulting from a changing climate itself. Both of these more specific definitions of radiative forcing have been widely adopted by the atmospheric science and climate communities. The most recent IPCC report (IPCC, 2013) also describes an alternate Effective Radiative Forcing (ERF), which allows physical variables (e.g. the temperature profile) "to respond to perturbations with rapid adjustments"; this does not include feedbacks or responses to climate change, but in the case of aerosols, now includes the "semi-direct effect" as a component of the ERF that describes aerosol-radiation interactions. The DRF includes both anthropogenic forcing driven by the rise in human emissions and land-use change as well natural forcing associated with changes in solar flux and volcanic emissions. This definition was somewhat confused by a second definition presented in the discussion of aerosol forcing in Sect. 2.4 of the 2007 IPCC report: "the direct RF only considers the anthropogenic components." There are very few natural aerosol forcers, with volcanoes, which are sporadic in nature and therefore difficult to compare with other forcers, as the primary example. Changes in natural aerosols are typically associated with climate feedbacks, such as changes brought on by changing temperatures or precipitation; for example increases in biogenic aerosol formation associated with temperature-

## Beyond direct radiative forcing

C. L. Heald et al.

[Title Page](#)

[Abstract](#)

[Introduction](#)

[Conclusions](#)

[References](#)

[Tables](#)

[Figures](#)

[|◀](#)

[▶|](#)

[◀](#)

[▶](#)

[Back](#)

[Close](#)

[Full Screen / Esc](#)

[Printer-friendly Version](#)

[Interactive Discussion](#)



driven increases in biogenic VOC emissions, or trends in dust emissions associated with changes in soil moisture or wind speed. However, anthropogenic land use change and anthropogenically-driven changes in the chemical environment can both affect natural aerosols, thus constituting a forcing ignored by this second, incomplete definition.

The DRF metric is relatively simple to estimate in atmospheric models (in that it does not require quantification of the climate response) and enables quantitative comparison of various anthropogenic forcing mechanisms on the Earth's energy budget. The aerosol DRF reflects both the change in primary aerosol emissions from anthropogenic activity and the impacts of the changing chemical environment (due to anthropogenic emissions) on secondary aerosol formation. The radiative impacts of natural aerosol are typically reflected in DRE, not DRF. Observations (from satellite or surface sun-photometers) characterize a total DRE of present-day aerosols; to estimate DRF the anthropogenic fraction is assumed (Yu et al., 2006). This distinction between DRE and DRF is sometimes confused in the literature (Jo et al., 2013; Heald et al., 2005; Liao et al., 2004; Kim et al., 2006; Artaxo et al., 2009; Massoli et al., 2009; Ma et al., 2012; Athanasopoulou et al., 2013; Goto et al., 2008), where the presence of any aerosol is assumed to imply a DRF. The radiative imbalance associated with the presence of these aerosols is only a DRF if pre-industrial concentrations were zero. However, the distinction between DRE and DRF remains somewhat murky, particularly when considering secondary aerosol formation. For example, changes in the chemical formation of biogenic secondary organic aerosol (SOA) due to changes in anthropogenic nitrogen oxide ( $\text{NO}_x$ ) emissions qualifies as a DRF, but similar changes induced by changes in lightning  $\text{NO}_x$  sources (due to a climate feedback) do not. In this study our objective is to quantify these two metrics, and make the case that the DRE is a necessary complement to the DRF for aerosols.

## Beyond direct radiative forcing

C. L. Heald et al.

[Title Page](#)

[Abstract](#)

[Introduction](#)

[Conclusions](#)

[References](#)

[Tables](#)

[Figures](#)

[|◀](#)

[▶|](#)

[Back](#)

[Close](#)

[Full Screen / Esc](#)

[Printer-friendly Version](#)

[Interactive Discussion](#)



## 2 Model description

Reducing the uncertainty associated with aerosol radiative forcing requires models that are well-tested against observations and that include the capacity to simulate radiative impacts. The temporal matching of observations and simulation, which is only possible  
5 using a chemical transport model (CTM) driven by assimilated meteorology (or a GCM nudged towards analyzed meteorology), is critical to the accurate evaluation of a simulation of short-lived species. Therefore, a CTM with an online coupled radiative transfer model is the most appropriate model configuration for consistently evaluating aerosol loading and direct radiative impacts.

We use here the fast radiation model RRTMG which we integrate online within the global GEOS-Chem chemical transport model ([www.geos-chem.org](http://www.geos-chem.org)), a configuration referred to as GCRT, to calculate the radiative fluxes associated with atmospheric aerosols. RRTMG uses the correlated-k method to calculate longwave (LW) and short-wave (SW) atmospheric fluxes. Further details on the aerosol simulation, emissions,  
10 optical properties, RRTMG, and the implementation in GEOS-Chem are provided in what follows.  
15

### 2.1 GEOS-Chem

We use v9-01-03 of GEOS-Chem driven by GEOS-5 assimilated meteorology from the Global Model and Assimilation Office for the year 2010 at a horizontal resolution of  
20  $2^\circ \times 2.5^\circ$  and 47 vertical levels.

The GEOS-Chem oxidant-aerosol simulation includes  $\text{H}_2\text{SO}_4\text{-HNO}_3\text{-NH}_3$  aerosol thermodynamics coupled to an ozone- $\text{NO}_x$ -hydrocarbon-aerosol chemical mechanism (Park et al., 2004, 2006). We use the standard bulk aerosol scheme, where all aerosols are described with one or more log-normal size bins. The ISORROPIA II thermodynamic equilibrium model (Fountoukis and Nenes, 2007) calculates the partitioning of total ammonia and nitric acid between the gas and particle (fine mode only) phases.  
25 The model scheme also includes organic aerosol (OA) and black carbon (BC) (Park

### Beyond direct radiative forcing

C. L. Heald et al.

[Title Page](#)

[Abstract](#)

[Introduction](#)

[Conclusions](#)

[References](#)

[Tables](#)

[Figures](#)

◀

▶

[Back](#)

[Close](#)

[Full Screen / Esc](#)

[Printer-friendly Version](#)

[Interactive Discussion](#)



**Beyond direct radiative forcing**

C. L. Heald et al.

[Title Page](#)[Abstract](#)[Introduction](#)[Conclusions](#)[References](#)[Tables](#)[Figures](#)[|◀](#)[▶|](#)[◀](#)[▶](#)[Back](#)[Close](#)[Full Screen / Esc](#)[Printer-friendly Version](#)[Interactive Discussion](#)

**Beyond direct radiative forcing**

C. L. Heald et al.

[Title Page](#)[Abstract](#)[Introduction](#)[Conclusions](#)[References](#)[Tables](#)[Figures](#)[|◀](#)[▶|](#)[◀](#)[▶](#)[Back](#)[Close](#)[Full Screen / Esc](#)[Printer-friendly Version](#)[Interactive Discussion](#)

Tropospheric methane concentrations are fixed at 2007 values from the NOAA CCGC cooperative air sampling network (4 latitude bands, mean concentrations ranging from 1733 to 1856 ppb).

Anthropogenic emissions of ozone and aerosol precursors ( $\text{SO}_x$ ,  $\text{NO}_x$ ,  $\text{NH}_3$ , BC, OC, CO, and VOCs) for the year 2100 follow the RCP 4.5 scenario as implemented by Holmes et al. (2013). These include fossil fuel, biofuel and agricultural emissions; all other natural and fire emissions, as well as methane concentrations, are identical in the 2100 and 2010 simulations performed here. We note that projections of aerosol precursor emissions show similar trajectories in all four of the RCP scenarios, with the exception of ammonia which is projected to remain reasonably constant in the RCP 4.5 scenario but projected to rise in all other scenarios. Global emission totals for aerosols and their precursors in 2010 and 2100 are given in Table 1.

Recent versions of the GEOS-Chem standard aerosol simulation have been extensively tested against airborne (van Donkelaar et al., 2008; Heald et al., 2011; Wang et al., 2011), shipborne (Lapina et al., 2011), and surface site (Zhang et al., 2012; Heald et al., 2012) mass concentration measurements as well as aerosol deposition measurements (Fisher et al., 2011) and satellite and ground-based observations of AOD (Ridley et al., 2012; Jaegle et al., 2010; Ford and Heald, 2012).

## 2.2 Rapid Radiative Transfer Model for GCMs (RRTMG)

RRTMG (Iacono et al., 2008) is a fast radiative transfer code that calculates longwave and shortwave atmospheric fluxes using the correlated-k method (Lacis and Oinas, 1991). This approach greatly increases computational speed while maintaining the effective accuracy of a line-by-line calculation. The absorption coefficients that are used to develop the code's k-distributions are attained directly from the Line-By-Line Radiative Transfer Model (LBLRTM) (Clough et al., 1992, 2005; Alvarado et al., 2013), which connects the spectroscopic foundation of RRTMG to high-spectral resolution validations done with atmospheric radiance observations. There are 16 bands in the longwave RRTMG code and 14 bands in the shortwave code (extending from 230 nm

through 56 µm); for boundaries see Mlawer et al. (1997) and Mlawer and Clough (1998). Modeled sources of extinction in RRTMG include H<sub>2</sub>O, O<sub>3</sub>, long-lived greenhouse gases, aerosols, ice and liquid clouds, and Rayleigh scattering. RRTMG has been successfully incorporated into a number of GCMs (Iacono et al., 2003, 2008), including the ECMWF IFS, the NCEP GFS and the NCAR CAM5.

For cloudy cases, vertical overlap of cloudy layers is handled using the Monte-Carlo Independent Column Approximation (McICA; Pincus et al., 2003), which reduces the computational load for the treatment of complex vertically overlapping cloud to that of a model run for a simpler configuration (e.g. clear, single-layer clouds) by assigning 5 statistically appropriate combinations of cloud layers to each spectral element in the calculation. This requires that comparisons between RRTMG and observed fluxes and heating rates average a sufficiently large number of data points (in space and/or time) to remove the unbiased noise introduced by the McICA approximation. This random noise in the radiative fluxes and heating rates introduced by McICA has been shown to 10 have statistically insignificant effects on GCM simulations (e.g. Barker et al., 2008).

RRTMG has been shown to be highly accurate in tests against reference radiative transfer calculations as part of the Continual Intercomparison of Radiation Codes (CIRC) project (Oreopoulos and Mlawer, 2010; Oreopoulos et al., 2012), which included numerous evaluations of the radiative effects due to aerosols.

## 20 2.3 Integration of GEOS-Chem and RRTMG (GCRT)

RRTMG is called at a user-specified temporal frequency (3 h here) within GEOS-Chem and calculates instantaneous radiative fluxes in both the shortwave and longwave. In addition to total fluxes, GCRT can calculate the SW or LW flux associated with a specific constituent of the troposphere (ozone, methane, sulfate, nitrate, ammonium, BC, OA, sea salt, dust or total particulate matter) by calling RRTMG again with zero constituent concentration for the species of interest and differencing the result. We describe the specification of a suite of relevant surface and atmospheric composition properties 25 here.

## Beyond direct radiative forcing

C. L. Heald et al.

[Title Page](#)

[Abstract](#)

[Introduction](#)

[Conclusions](#)

[References](#)

[Tables](#)

[Figures](#)

[◀](#)

[▶](#)

[Back](#)

[Close](#)

[Full Screen / Esc](#)

[Printer-friendly Version](#)

[Interactive Discussion](#)



All aerosols in GEOS-Chem are treated as externally mixed with log-normal size distributions and optical properties (including refractive indices and growth factors) defined by the Global Aerosol Data Set (GADS) database (Kopke et al., 1997), with recent updates (Drury et al., 2010; Jaegle et al., 2010; Ridley et al., 2012). We update  
5 the BC density and refractive index to follow recommendations of Bond and Bergstrom (2006) and the shortwave refractive indices for dust following Sinyuk (2003). We also link simulated sulfate with the GADS water soluble aerosol properties, not the sulfuric acid properties previously applied in the GEOS-Chem simulation, as recommended by Hess et al. (1998). Table 2 gives the relevant optical and size properties for dry  
10 aerosol. Mie code is used to calculate the resulting optical properties (including mass extinction efficiency) at 7 discrete relative humidities (RH) for each wavelength. The optical properties generated at 61 GADS wavelengths (from 250 nm to 40  $\mu\text{m}$ ) are spline interpolated to the 30 RRTMG wavelengths (230 nm to 56  $\mu\text{m}$ ) and stored in a look-up table which includes the mass extinction efficiency, the single scattering albedo (SSA)  
15 and asymmetry parameter ( $g$ ). Aerosol properties at the two RRTMG wavelengths that fall outside of the range of the GADS wavelengths are fixed at the values of the shortest and longest wavelengths in GADS. The AOD at a specific wavelength is calculated within GEOS-Chem as a function of local relative humidity from the mass concentration and mass extinction efficiency according to the formulation of Tegen and Lacis  
20 (1996). RRTMG uses the AOD, SSA and asymmetry parameter for each aerosol type to calculate aerosol impacts on radiative fluxes in both the shortwave and longwave.

Vertical profiles of a suite of greenhouse gases are fixed in GCRT for both longwave and shortwave flux calculations. These include:  $\text{N}_2\text{O}$  and stratospheric  $\text{CH}_4$  (following July 2012 zonal mean climatology from the TES instrument), CFCs (CFC-11, CFC-12,  
25 and CCl<sub>4</sub> from UARS climatology and CFC-22 from the MIPAS climatology, all scaled to match surface values provided in IPCC, 2007) and  $\text{CO}_2$  (set to 390 ppm globally). Zonally averaged tropospheric methane concentrations are fixed as described in Sect. 2.1. Tropospheric ozone is simulated interactively in GEOS-Chem; stratospheric concentrations are calculated based on the method used in FAST-J (Wild et al., 2000). Water

## Beyond direct radiative forcing

C. L. Heald et al.

[Title Page](#)

[Abstract](#)

[Introduction](#)

[Conclusions](#)

[References](#)

[Tables](#)

[Figures](#)

[|◀](#)

[▶|](#)

[Back](#)

[Close](#)

[Full Screen / Esc](#)

[Printer-friendly Version](#)

[Interactive Discussion](#)



**Beyond direct radiative forcing**

C. L. Heald et al.

[Title Page](#)[Abstract](#)[Introduction](#)[Conclusions](#)[References](#)[Tables](#)[Figures](#)[|◀](#)[▶|](#)[Back](#)[Close](#)[Full Screen / Esc](#)[Printer-friendly Version](#)[Interactive Discussion](#)

### 3 Results

## Beyond direct radiative forcing

C. L. Heald et al.

[Title Page](#)

[Abstract](#)

[Introduction](#)

[Conclusions](#)

[References](#)

[Tables](#)

[Figures](#)

[◀](#)

[▶](#)

[◀](#)

[▶](#)

[Back](#)

[Close](#)

[Full Screen / Esc](#)

[Printer-friendly Version](#)

[Interactive Discussion](#)



in situ observations (Jaegle et al., 2010). The calculated global mean mass extinction efficiency (MEE) for all aerosol are lower than the AeroCom II model means, however the wide range of model estimates given by Myhre et al. (2013) suggests that these are not well constrained in the AeroCom II models. In fact this large range in model MEE suggests that differences in model treatments of aerosol removal, size, and optical properties (including water uptake) can lead to at least a factor of two difference in model estimates of aerosol radiative fluxes.

Lower aerosol MEE in GCRT translate to a lower global mean mid-visible AOD of 0.092 compared to the AeroCom I model mean of 0.127 and satellite-based estimates (~ 0.15) (Kinne et al., 2006). Figure 2 shows the geographical distribution of annual mean AOD for present-day, over half of which is attributed to dust and sea salt. Sulfate and OA contribute a further 33 %, with nitrate, ammonium and BC making minor near-source contributions to the global AOD. The GCRT anthropogenic AOD is 77 % of the mean of the AeroCom II models. Similarly, the GCRT estimate of clear-sky ( $-0.57 \text{ Wm}^{-2}$ ) global mean TOA aerosol direct radiative forcing (DRF) is 15 % lower (less cooling) than the AeroCom II model mean.

The IPCC (2007) estimates the aerosol DRF at  $-0.5 \text{ Wm}^{-2}$  (with a range of  $-0.9$  to  $-0.1 \text{ Wm}^{-2}$ ) in 2005 based on both models and satellite measurement. The model-only value (adjusted for dust and nitrate which is not included in all models) is lower at  $-0.4 \text{ Wm}^{-2}$ . Our global-mean all-sky value for 2010 ( $-0.36 \text{ Wm}^{-2}$ ) is similar. We do not include any biomass burning sources in our DRF calculation due to the uncertainty in attributing the anthropogenic fraction. Anthropogenic modulation of biomass burning emissions is driven by changing agricultural practices, land clearing, and human fire suppression but not by climate change (this constitutes a feedback). We use an additional simulation to estimate a DRE of  $-0.19 \text{ Wm}^{-2}$  from all biomass burning particles in 2010 ( $-0.23 \text{ Wm}^{-2}$  from OA,  $+0.06 \text{ Wm}^{-2}$  from BC and  $-0.02 \text{ Wm}^{-2}$  from inorganic aerosol). The IPCC (2007) estimate of the aerosol DRF of biomass burning linked with human activities is  $+0.03 \text{ Wm}^{-2}$ , indicating that the net impact of biomass burning aerosol is treated as more absorbing than our estimate or that the amount and

Beyond direct radiative forcing

C. L. Heald et al.

[Title Page](#)

[Abstract](#)

[Introduction](#)

[Conclusions](#)

[References](#)

[Tables](#)

[Figures](#)

[|◀](#)

[▶|](#)

[◀](#)

[▶](#)

[Back](#)

[Close](#)

[Full Screen / Esc](#)

[Printer-friendly Version](#)

[Interactive Discussion](#)



spatial distribution of the aerosol relative to underlying reflecting clouds and areas with high surface albedo differ.

All-sky DRF in GCRT is 63 % of the estimate of clear-sky DRF. The global annual mean cloud fraction in GCRT for 2010 is 60 %. This implies a global-mean cloud-sky TOA DRF of  $-0.22 \text{ Wm}^{-2}$ , a lower value (less cooling), consistent with a shading of scattering aerosols below-clouds and enhanced absorption from BC above clouds. The all-sky to clear-sky ratio is typically  $\sim 50\%$  for the AeroCom II models (Myhre et al., 2013). Our slightly higher fraction is likely the result of the lower estimated BC loading.

Table 3 shows that the total TOA radiative effects are dominated by aerosol impacts in the shortwave (visible-UV) wavelengths, where they reflect solar radiation and cool the Earth (with the exception of BC which absorbs solar radiation). Modest warming ( $< 10\%$  of the cooling effect) results from scattering (by large particles such as dust) or absorption in the longwave (IR) wavelengths (Fig. 2). This indicates that a SW-only aerosol DRE or DRF estimate would overestimate the cooling effect by  $\sim 5\text{--}10\%$ .

Figure 3 contrasts the GCRT estimates of all-sky DRF and DRE. The DRF represents a change in radiative balance from pre-industrial to present-day (2010) with fixed climate, which reflects the rise in anthropogenic emissions (and anthropogenic land use, not considered here). Conversely, the DRE represents the total present-day radiative impact from all aerosols in the atmosphere, including those of natural origin. As a result, aerosols that are dominated by anthropogenic sources (e.g. nitrate) show a similar DRE and DRF, whereas natural aerosols (e.g. sea salt) have a large DRE but zero DRF. The estimate of total aerosol DRE ( $-1.83 \text{ Wm}^{-2}$ ) is more than 5 times the value of the DRF ( $-0.36 \text{ Wm}^{-2}$ ) in 2010, thus the global radiative impact of “natural” aerosol is more than 4 times that of anthropogenic aerosol perturbation. Rap et al. (2013) estimated an all-sky natural aerosol DRE of  $-0.81 \text{ Wm}^{-2}$  from DMS-sulfate, sea-salt, terpene SOA and wildfire alone.

Figure 4 shows the zonal distribution of the GCRT simulated radiative impacts. We see that the forcing is highly concentrated at Northern mid-latitudes, driven by anthro-

## Beyond direct radiative forcing

C. L. Heald et al.

[Title Page](#)

[Abstract](#)

[Introduction](#)

[Conclusions](#)

[References](#)

[Tables](#)

[Figures](#)

[◀](#)

[▶](#)

[Back](#)

[Close](#)

[Full Screen / Esc](#)

[Printer-friendly Version](#)

[Interactive Discussion](#)



pogenic emissions in North America, Europe and Asia, in agreement with previous model studies (Myhre et al., 2013). Modest radiative impacts in the Arctic are the result of spring/summer Eurasian sulfate pollution, during seasons of minimum snow cover. Conversely, the DRE is distributed throughout the world with maxima associated with not only anthropogenic emissions in the NH, but also with sea salt emissions in the Southern Ocean, biomass burning in the tropics and Arctic, and dust from Africa and Asia. Warming dominates over the highly reflective desert regions in the Saharan desert, the Middle East and high Northern latitudes; shortwave scattering prevails in all other regions in the simulation.

Similarly, Fig. 5 shows that the global mean DRF from aerosols is largest in boreal springtime, whereas the DRE is more uniform throughout the year, with summertime peaks due to OA compensated by wintertime enhancements in ammonium nitrate and sea salt.

Figure 3 also shows an estimate of the aerosol all-sky DRF in 2100 from a GCRT simulation based on the RCP 4.5 emissions scenario. Due to the steep decline in  $\text{SO}_2$  emissions (Table 1), the global mean sulfate DRF drops by ~85 % from 2010 to  $-0.031 \text{ Wm}^{-2}$ . As shown by Pinder et al. (2007), reductions in sulfate can lead to enhanced ammonium nitrate formation in environments with abundant ammonia supply. Given that ammonia emissions in 2100 are predicted to be approximately equivalent to those in 2010 in the RCP4.5 scenario, nitrate DRF in 2100 increases by 60 % to  $-0.088 \text{ Wm}^{-2}$ . Overall forcing from ammonium decreases (the decline in ammonium sulfate outweighing the increase in ammonium nitrate) to  $-0.046 \text{ Wm}^{-2}$ . Finally, changes in BC and POA are more modest, but the magnitude of DRF decreases for both (to 0.056 and  $-0.053 \text{ Wm}^{-2}$  respectively). Dust forcing is maintained at 2010 values. Overall the clear-sky TOA DRF in 2100 ( $-0.22 \text{ Wm}^{-2}$ ) drops by 39 % from 2010. Smith and Bond (2013) also estimate a precipitous decline (62 %) in aerosol (carbonaceous and sulfate only) radiative forcing from 2000 to 2100 when including both the direct and indirect forcing.

Beyond direct radiative forcing

C. L. Heald et al.

[Title Page](#)

[Abstract](#)

[Introduction](#)

[Conclusions](#)

[References](#)

[Tables](#)

[Figures](#)

[◀](#)

[▶](#)

[Back](#)

[Close](#)

[Full Screen / Esc](#)

[Printer-friendly Version](#)

[Interactive Discussion](#)



## Beyond direct radiative forcing

C. L. Heald et al.

[Title Page](#)

[Abstract](#)

[Introduction](#)

[Conclusions](#)

[References](#)

[Tables](#)

[Figures](#)

[|◀](#)

[▶|](#)

[◀](#)

[▶](#)

[Back](#)

[Close](#)

[Full Screen / Esc](#)

[Printer-friendly Version](#)

[Interactive Discussion](#)



Uncertainty in our estimates of DRF are dominated by the uncertainty in the MEE (as shown by the AeroCom II study of Myhre et al., 2013). Assumptions regarding size, water uptake and absorption efficiency (e.g. the prevalence of brown carbon, Andreae and Gelencser, 2006) all contribute to this. We do not treat absorption enhancement from the coating of BC (Jacobson, 2000), the importance of which is unclear (Cappa et al., 2012; Lack et al., 2012), therefore both DRE and DRF values may underestimate absorption. In addition to the uncertainty associated with aerosol optics, our simulations likely underestimate the “anthropogenically-controlled” SOA in the atmosphere, which is estimated to contribute  $-0.26 \text{ W m}^{-2}$  of direct cooling (Spracklen et al., 2011). The global source of dust arising from anthropogenic activity is also poorly constrained.

Uncertainties in our estimate of DRE are likely even larger than uncertainties on DRF. This is the result of: (1) better constraints on anthropogenic sectoral emissions (e.g. mobile sources, power generation), (2) a poor understanding of natural particle emissions from ecosystems, both marine and terrestrial (e.g. terrestrial primary biological aerosol particles (e.g. Heald and Spracklen, 2009), marine OA and methane sulfonate (Heintzenberg et al., 2000) – none of which are included in this GCRT simulation) and (3) the geographical extent and remoteness of regions impacted by natural aerosols and hence a lack of measurement constraint (and thus well-tested models).

## 4 Discussion and conclusions

We use the newly online coupled GEOS-Chem-RRTMG (GCRT) global model to estimate the direct radiative effect and direct radiative forcing of atmospheric aerosols. The global TOA DRE is over five times the cooling estimated as the DRF. This illustrates that tropospheric aerosols exert a large influence on the global energy balance. However, the quantification of DRE and DRF is highly uncertain and the estimate of the ratio between them is specific to this model configuration and the concurrent assumptions. While the aerosol burden in the GEOS-Chem model is well-tested against observations (e.g. Zhang et al., 2012; Fisher et al., 2011; Ridley et al., 2012; Jaegle

**Beyond direct radiative forcing**

C. L. Heald et al.

[Title Page](#)[Abstract](#)[Introduction](#)[Conclusions](#)[References](#)[Tables](#)[Figures](#)[|◀](#)[▶|](#)[◀](#)[▶](#)[Back](#)[Close](#)[Full Screen / Esc](#)[Printer-friendly Version](#)[Interactive Discussion](#)

“climate change may alter natural aerosol sources as well as removal by precipitation”. Carslaw et al. (2010) suggest that changes in natural aerosols, largely driven by climate feedbacks may result in radiative perturbations of up to  $\pm 1 \text{ W m}^{-2}$ . It is therefore critical that we expand our set of metrics to address the many factors that the DRF neglects by design. Figure 6b shows a more comprehensive set of drivers for changing aerosol abundance, including climate feedbacks and natural emissions. In addition to the direct effect of aerosols on climate (the focus of this study), the indirect effects of aerosols, both the conventional aerosol–cloud interactions and the less-well constrained effect of aerosols on biogeochemistry (Mahowald, 2011), can feedback on aerosol abundance via climate impacts. The relative importance of these feedbacks and forcings on the global radiative flux imbalance over time is unclear and deserves further investigation. The challenge of attributing a feedback is also non-trivial (e.g. to what agent does one associate a temperature-driven change in aerosol abundance?). Inherently, the calculation of DRE over time (with varying climate) includes the potential to quantify (though not attribute) these effects. Furthermore, estimates of the aerosol indirect effect are very sensitive to the pre-industrial aerosol burden (Menon et al., 2002), for which little observational constraint exists. Thus, two climate models with identical aerosol DRFs could provide very different estimates of the aerosol indirect aerosol forcing due to differences in the pre-industrial (natural) aerosol burden. Comparing the pre-industrial DRE simulated in models would provide a first step towards identifying these key differences.

Quantifying and reporting the instantaneous DRE in global models is a simple and necessary first step in going beyond the DRF metric for aerosols. While it may not directly serve as a policy tool, the DRE is more easily tested against observations (e.g. satellites), is a more thorough gauge for model comparisons, and offers a more complete picture of aerosols in the climate system. As such, it is an important complement to the DRF for advancing our understanding and predictions of the global aerosol burden and how it may counteract future trends in greenhouse gas warming.

Beyond direct radiative forcing

C. L. Heald et al.

[Title Page](#)

[Abstract](#)

[Introduction](#)

[Conclusions](#)

[References](#)

[Tables](#)

[Figures](#)

[|◀](#)

[▶|](#)

[◀](#)

[▶](#)

[Back](#)

[Close](#)

[Full Screen / Esc](#)

[Printer-friendly Version](#)

[Interactive Discussion](#)



*Acknowledgements.* This work was supported by the EPA-STAR program and the Charles E. Reed Faculty Initiative Fund. Although the research described in this article has been funded in part by the US EPA through grant/cooperative agreement (RD-83503301), it has not been subjected to the Agency's required peer and policy review and therefore does not necessarily reflect the views of the Agency and no official endorsement should be inferred.

## References

- Alexander, B., Park, R. J., Jacob, D. J., Li, Q. B., Yantosca, R. M., Savarino, J., Lee, C. C. W., and Thiemens, M. H.: Sulfate formation in sea-salt aerosols: constraints from oxygen isotopes, *J. Geophys. Res.-Atmos.*, 110, D10307, doi:10.1029/2004JD005659, 2005.
- Alvarado, M. J., Payne, V. H., Mlawer, E. J., Uymin, G., Shephard, M. W., Cady-Pereira, K. E., Delamere, J. S., and Moncet, J.-L.: Performance of the Line-By-Line Radiative Transfer Model (LBLRTM) for temperature, water vapor, and trace gas retrievals: recent updates evaluated with IASI case studies, *Atmos. Chem. Phys.*, 13, 6687–6711, doi:10.5194/acp-13-6687-2013, 2013.
- Andreae, M. O. and Gelencsér, A.: Black carbon or brown carbon? The nature of light-absorbing carbonaceous aerosols, *Atmos. Chem. Phys.*, 6, 3131–3148, doi:10.5194/acp-6-3131-2006, 2006.
- Artaxo, P., Rizzo, L. V., Paixao, M., de Lucca, S., Oliveira, P. H., Lara, L. L., Wiedemann, K. T., Andreae, M. O., Holben, B., Schafer, J., Correia, A. L., and Pauliquevis, T. M.: Aerosol particles in Amazonia: their composition, role in the radiation balance, cloud formation, and nutrient cycles, in: *Amazonia and Global Change*, *Geoph. Monog. Series*, 233–250, 2009.
- Athanasiopoulou, E., Vogel, H., Vogel, B., Tsimpidi, A. P., Pandis, S. N., Knote, C., and Fountoukis, C.: Modeling the meteorological and chemical effects of secondary organic aerosols during an EUCAARI campaign, *Atmos. Chem. Phys.*, 13, 625–645, doi:10.5194/acp-13-625-2013, 2013.
- Barker, H. W., Cole, J. N. S., Morcrette, J. J., Pincus, R., Raisaenen, P., von Salzen, K., and Vaillancourt, P. A.: The Monte Carlo Independent Column Approximation: an assessment using several global atmospheric models, *Q. J. Roy. Meteor. Soc.*, 134, 1463–1478, doi:10.1002/qj.303, 2008.

[Title Page](#)

[Abstract](#)

[Introduction](#)

[Conclusions](#)

[References](#)

[Tables](#)

[Figures](#)

[◀](#)

[▶](#)

[Back](#)

[Close](#)

[Full Screen / Esc](#)

[Printer-friendly Version](#)

[Interactive Discussion](#)



- Bond, T. C. and Bergstrom, R. W.: Light absorption by carbonaceous particles: an investigative review, *Aerosol Sci. Tech.*, 40, 27–67, doi:10.1080/02786820500421521, 2006.
- Bond, T. C., Bhardwaj, E., Dong, R., Jogani, R., Jung, S. K., Roden, C., Streets, D. G., and Trautmann, N. M.: Historical emissions of black and organic carbon aerosol from energy-related combustion, 1850–2000, *Glob. Biogeochem. Cycle*, 21, 16, Gb2018, doi:10.1029/2006gb002840, 2007.
- Bouwman, A. F., Lee, D. S., Asman, W. A. H., Dentener, F. J., VanderHoek, K. W., and Olivier, J. G. J.: A global high-resolution emission inventory for ammonia, *Glob. Biogeochem. Cycle*, 11, 561–587, 1997.
- Cappa, C. D., Onasch, T. B., Massoli, P., Worsnop, D. R., Bates, T. S., Cross, E. S., Davidovits, P., Hakala, J., Hayden, K. L., Jobson, B. T., Kolesar, K. R., Lack, D. A., Lerner, B. M., Li, S. M., Mellon, D., Nuaaman, I., Olfert, J. S., Petaja, T., Quinn, P. K., Song, C., Subramanian, R., Williams, E. J., and Zaveri, R. A.: Radiative absorption enhancements due to the mixing state of atmospheric black carbon, *Science*, 337, 1078–1081, doi:10.1126/science.1223447, 2012.
- Carslaw, K. S., Boucher, O., Spracklen, D. V., Mann, G. W., Rae, J. G. L., Woodward, S., and Kulmala, M.: A review of natural aerosol interactions and feedbacks within the Earth system, *Atmos. Chem. Phys.*, 10, 1701–1737, doi:10.5194/acp-10-1701-2010, 2010.
- Chung, S. H. and Seinfeld, J. H.: Global distribution and climate forcing of carbonaceous aerosols, *J. Geophys. Res.-Atmos.*, 107, 4407, doi:10.1029/2001JD001397, 2002.
- Clough, S. A., Iacono, M. J., and Moncet, J. L.: Line-by-line calculations of atmospheric fluxes and cooling rates – application to water-vapor, *J. Geophys. Res.-Atmos.*, 97, 15761–15785, 1992.
- Clough, S. A., Shephard, M. W., Mlawer, E., Delamere, J. S., Iacono, M., Cady-Pereira, K., Boukabara, S., and Brown, P. D.: Atmospheric radiative transfer modeling: a summary of the AER codes, *J. Quant. Spectrosc. Radiat. Transf.*, 91, 233–244, doi:10.1016/j.jqsrt.2004.05.058, 2005.
- Drury, E. E., Jacob, D. J., Spurr, R. J. D., Wang, J., Shinozuka, Y., Anderson, B. E., Clarke, A. D., Dibb, J., McNaughton, C., and Weber, R. J.: Synthesis of satellite (MODIS), aircraft (ICARTT), and surface (IMPROVE, EPA-AQS, AERONET) aerosol observations over eastern North America to improve MODIS aerosol retrievals and constrain aerosol concentrations and sources, *J. Geophys. Res.-Atmos.*, 115, D14204, doi:10.1029/2009JD012629, 2010.

Beyond direct radiative forcing

C. L. Heald et al.

[Title Page](#)

[Abstract](#)

[Introduction](#)

[Conclusions](#)

[References](#)

[Tables](#)

[Figures](#)

◀

▶

◀

▶

[Back](#)

[Close](#)

[Full Screen / Esc](#)

[Printer-friendly Version](#)

[Interactive Discussion](#)



**Beyond direct radiative forcing**

C. L. Heald et al.

[Title Page](#)[Abstract](#)[Introduction](#)[Conclusions](#)[References](#)[Tables](#)[Figures](#)[|◀](#)[▶|](#)[◀](#)[▶](#)[Back](#)[Close](#)[Full Screen / Esc](#)[Printer-friendly Version](#)[Interactive Discussion](#)

- Heald, C. L., Jacob, D. J., Park, R. J., Russell, L. M., Huebert, B. J., Seinfeld, J. H., Liao, H., and Weber, R. J.: A large organic aerosol source in the free troposphere missing from current models, *Geophys. Res. Lett.*, 32, L18809, doi:10.1029/2005GL023831, 2005.
- Heald, C. L., Wilkinson, M. J., Monson, R. K., Alo, C. A., Wang, G. L., and Guenther, A.: Response of isoprene emission to ambient CO<sub>2</sub> changes and implications for global budgets, *Glob. Change Biol.*, 15, 1127–1140, doi:10.1111/j.1365-2486.2008.01802.x, 2009.
- Heald, C. L., Coe, H., Jimenez, J. L., Weber, R. J., Bahreini, R., Middlebrook, A. M., Russell, L. M., Jolley, M., Fu, T.-M., Allan, J. D., Bower, K. N., Capes, G., Crosier, J., Morgan, W. T., Robinson, N. H., Williams, P. I., Cubison, M. J., DeCarlo, P. F., and Dunlea, E. J.: Exploring the vertical profile of atmospheric organic aerosol: comparing 17 aircraft field campaigns with a global model, *Atmos. Chem. Phys.*, 11, 12673–12696, doi:10.5194/acp-11-12673-2011, 2011.
- Heald, C. L., J. L. Collett Jr., Lee, T., Benedict, K. B., Schwandner, F. M., Li, Y., Clarisse, L., Hurtmans, D. R., Van Damme, M., Clerbaux, C., Coheur, P.-F., Philip, S., Martin, R. V., and Pye, H. O. T.: Atmospheric ammonia and particulate inorganic nitrogen over the United States, *Atmos. Chem. Phys.*, 12, 10295–10312, doi:10.5194/acp-12-10295-2012, 2012.
- Heintzenberg, J., Covert, D. C., and Van Dingenen, R.: Size distribution and chemical composition of marine aerosols: a compilation and review, *Tellus B*, 52, 1104–1122, doi:10.1034/j.1600-0889.2000.00136.x, 2000.
- Henze, D. K. and Seinfeld, J. H.: Global secondary organic aerosol from isoprene oxidation, *Geophys. Res. Lett.*, 33, L09812, doi:10.1029/2006GL025976, 2006.
- Henze, D. K., Seinfeld, J. H., Ng, N. L., Kroll, J. H., Fu, T.-M., Jacob, D. J., and Heald, C. L.: Global modeling of secondary organic aerosol formation from aromatic hydrocarbons: high- vs. low-yield pathways, *Atmos. Chem. Phys.*, 8, 2405–2420, doi:10.5194/acp-8-2405-2008, 2008.
- Hess, M., Koepke, P., and Schult, I.: Optical properties of aerosols and clouds: the software package OPAC, *B. Am. Meteorol. Soc.*, 79, 831–844, 1998.
- Holmes, C. D., Prather, M. J., Søvde, O. A., and Myhre, G.: Future methane, hydroxyl, and their uncertainties: key climate and emission parameters for future predictions, *Atmos. Chem. Phys.*, 13, 285–302, doi:10.5194/acp-13-285-2013, 2013.
- Hu, Y. X. and Stamnes, K.: An accurate parameterization of the radiative properties of water clouds suitable for use in climate models, *J. Climate.*, 6, 728–742, doi:10.1175/1520-0442(1993)006<0728:AAPOTR>2.0.CO;2, 1993.

**Beyond direct radiative forcing**

C. L. Heald et al.

[Title Page](#)[Abstract](#)[Introduction](#)[Conclusions](#)[References](#)[Tables](#)[Figures](#)[|◀](#)[▶|](#)[◀](#)[▶](#)[Back](#)[Close](#)[Full Screen / Esc](#)[Printer-friendly Version](#)[Interactive Discussion](#)

**Beyond direct radiative forcing**

C. L. Heald et al.

[Title Page](#)[Abstract](#)[Introduction](#)[Conclusions](#)[References](#)[Tables](#)[Figures](#)[|◀](#)[▶|](#)[◀](#)[▶](#)[Back](#)[Close](#)[Full Screen / Esc](#)[Printer-friendly Version](#)[Interactive Discussion](#)

Koch, D., Schulz, M., Kinne, S., McNaughton, C., Spackman, J. R., Balkanski, Y., Bauer, S., Berntsen, T., Bond, T. C., Boucher, O., Chin, M., Clarke, A., De Luca, N., Dentener, F., Diehl, T., Dubovik, O., Easter, R., Fahey, D. W., Feichter, J., Fillmore, D., Freitag, S., Ghan, S., Ginoux, P., Gong, S., Horowitz, L., Iversen, T., Kirkevåg, A., Klimont, Z., Kondo, Y., Krol, M., Liu, X., Miller, R., Montanaro, V., Moteki, N., Myhre, G., Penner, J. E., Perlitz, J., Pitari, G., Reddy, S., Sahu, L., Sakamoto, H., Schuster, G., Schwarz, J. P., Seland, Ø., Stier, P., Takegawa, N., Takemura, T., Textor, C., van Aardenne, J. A., and Zhao, Y.: Evaluation of black carbon estimations in global aerosol models, *Atmos. Chem. Phys.*, 9, 9001–9026, doi:10.5194/acp-9-9001-2009, 2009.

Kopke, P., Hess, M., Schult, I., and Shettle, E. P.: Global Aerosol Data Set, Max Planck Inst. fur Meteorol., Hamburg, Germany, 1997.

Lacis, A. A. and Oinas, V.: A description of the correlated kappa-distribution method for modeling nongray gaseous absorption, thermal emission, and multiple-scattering in vertically inhomogeneous atmosphere *J. Geophys. Res.-Atmos.*, 96, 9027–9063, doi:10.1029/90jd01945, 1991.

Lack, D. A., Langridge, J. M., Bahreini, R., Cappa, C. D., Middlebrook, A. M., and Schwarz, J. P.: Brown carbon and internal mixing in biomass burning particles, *P. Natl. Acad. Sci. USA*, 109, 14802–14807, doi:10.1073/pnas.1206575109, 2012.

Lapina, K., Heald, C. L., Spracklen, D. V., Arnold, S. R., Allan, J. D., Coe, H., McFig-gans, G., Zorn, S. R., Drewnick, F., Bates, T. S., Hawkins, L. N., Russell, L. M., Smirnov, A., O'Dowd, C. D., and Hind, A. J.: Investigating organic aerosol loading in the remote marine environment, *Atmos. Chem. Phys.*, 11, 8847–8860, doi:10.5194/acp-11-8847-2011, 2011.

Liao, H., Seinfeld, J. H., Adams, P. J., and Mickley, L. J.: Global radiative forcing of coupled tropospheric ozone and aerosols in a unified general circulation model, *J. Geophys. Res.-Atmos.*, 109, D16207, doi:10.1029/2003jd004456, 2004.

Liu, H. Y., Jacob, D. J., Bey, I., and Yantosca, R. M.: Constraints from Pb-210 and Be-7 on wet deposition and transport in a global three-dimensional chemical tracer model driven by assimilated meteorological fields, *J. Geophys. Res.-Atmos.*, 106, 12109–12128, 2001.

Ma, X., Yu, F., and Luo, G.: Aerosol direct radiative forcing based on GEOS-Chem-APM and uncertainties, *Atmos. Chem. Phys.*, 12, 5563–5581, doi:10.5194/acp-12-5563-2012, 2012.

## Beyond direct radiative forcing

C. L. Heald et al.

[Title Page](#)

[Abstract](#)

[Introduction](#)

[Conclusions](#)

[References](#)

[Tables](#)

[Figures](#)

◀

▶

◀

▶

[Back](#)

[Close](#)

[Full Screen / Esc](#)

[Printer-friendly Version](#)

[Interactive Discussion](#)



- Mahowald, N.: Aerosol indirect effect on biogeochemical cycles and climate, *Science*, 334, 794–796, doi:10.1126/science.1207374, 2011.
- Mahowald, N. M. and Luo, C.: A less dusty future?, *Geophys. Res. Lett.*, 30, 4, 1903, doi:10.1029/2003gl017880, 2003.
- Massoli, P., Bates, T. S., Quinn, P. K., Lack, D. A., Baynard, T., Lerner, B. M., Tucker, S. C., Brioude, J., Stohl, A., and Williams, E. J.: Aerosol optical and hygroscopic properties during TexAQS-GoMACCS 2006 and their impact on aerosol direct radiative forcing, *J. Geophys. Res.-Atmos.*, 114, D00f07, doi:10.1029/2008jd011604, 2009.
- Menon, S., Del Genio, A. D., Koch, D., and Tselioudis, G.: GCM Simulations of the aerosol indirect effect: sensitivity to cloud parameterization and aerosol burden, *J. Atmos. Sci.*, 59, 692–713, doi:10.1175/1520-0469(2002)059<0692:gsotai>2.0.co;2, 2002.
- Mlawer, E. J. and Clough, S. A.: Shortwave and longwave enhancements in the rapid radiative transfer model, 7th Atmospheric Radiation Measurement (ARM) Science Team Meeting, San Antonia, Texas, 3–7 March 1997, 409–413, 1998.
- Mlawer, E. J., Taubman, S. J., Brown, P. D., Iacono, M. J., and Clough, S. A.: Radiative transfer for inhomogeneous atmospheres: RRTM, a validated correlated-k model for the longwave, *J. Geophys. Res.-Atmos.*, 102, 16663–16682, doi:10.1029/97jd00237, 1997.
- Myhre, G., Samset, B. H., Schulz, M., Balkanski, Y., Bauer, S., Berntsen, T. K., Bian, H., Bellouin, N., Chin, M., Diehl, T., Easter, R. C., Feichter, J., Ghan, S. J., Hauglustaine, D., Iversen, T., Kinne, S., Kirkevåg, A., Lamarque, J.-F., Lin, G., Liu, X., Lund, M. T., Luo, G., Ma, X., van Noije, T., Penner, J. E., Rasch, P. J., Ruiz, A., Selander, Ø., Skeie, R. B., Stier, P., Takemura, T., Tsigaridis, K., Wang, P., Wang, Z., Xu, L., Yu, H., Yu, F., Yoon, J.-H., Zhang, K., Zhang, H., and Zhou, C.: Radiative forcing of the direct aerosol effect from AeroCom Phase II simulations, *Atmos. Chem. Phys.*, 13, 1853–1877, doi:10.5194/acp-13-1853-2013, 2013.
- Olivier, J. G. J., Berdowski, J. J. M., Peters, J. A. H. W., Bakker, J., Visschedijk, A. J. H., and Bloos, J.-P. J.: Applications of EDGAR Including a description of EDGAR 3.0: reference database with trend data for 1970–1995, Natl. Inst. of Public Health and Environ., Bilthoven, the Netherlands, 2001.
- Oreopoulos, L. and Mlawer, E.: The Continual Intercomparison of Radiation Codes (CIRC) assessing anew the quality of GCM Radiation Algorithms, *B. Am. Meteorol. Soc.*, 91, 305–310, doi:10.1175/2009bams2732.1, 2010.
- Oreopoulos, L., Mlawer, E., Delamere, J., Shippert, T., Cole, J., Fomin, B., Iacono, M., Jin, Z. H., Li, J. N., Manners, J., Raisanen, P., Rose, F., Zhang, Y. C., Wilson, M. J., and Rossow, W. B.:

Beyond direct radiative forcing

C. L. Heald et al.

Title Page

Abstract

Introduction

Conclusions

References

Tables

Figures

◀

▶

Back

Close

Full Screen / Esc

Printer-friendly Version

Interactive Discussion



**Beyond direct radiative forcing**

C. L. Heald et al.

[Title Page](#)[Abstract](#)[Introduction](#)[Conclusions](#)[References](#)[Tables](#)[Figures](#)[|◀](#)[▶|](#)[◀](#)[▶](#)[Back](#)[Close](#)[Full Screen / Esc](#)[Printer-friendly Version](#)[Interactive Discussion](#)

**Beyond direct radiative forcing**

C. L. Heald et al.

[Title Page](#)[Abstract](#)[Introduction](#)[Conclusions](#)[References](#)[Tables](#)[Figures](#)[|◀](#)[▶|](#)[◀](#)[▶](#)[Back](#)[Close](#)[Full Screen / Esc](#)[Printer-friendly Version](#)[Interactive Discussion](#)

- Tegen, I., Werner, M., Harrison, S. P., and Kohfeld, K. E.: Relative importance of climate and land use in determining present and future global soil dust emission, *Geophys. Res. Lett.*, 31, 4, L05105, doi:10.1029/2003gl019216, 2004.
- van der Werf, G. R., Randerson, J. T., Giglio, L., Collatz, G. J., Mu, M., Kasibhatla, P. S., Morton, D. C., DeFries, R. S., Jin, Y., and van Leeuwen, T. T.: Global fire emissions and the contribution of deforestation, savanna, forest, agricultural, and peat fires (1997–2009), *Atmos. Chem. Phys.*, 10, 11707–11735, doi:10.5194/acp-10-11707-2010, 2010.
- van Donkelaar, A., Martin, R. V., Leaitch, W. R., Macdonald, A. M., Walker, T. W., Streets, D. G., Zhang, Q., Dunlea, E. J., Jimenez, J. L., Dibb, J. E., Huey, L. G., Weber, R., and Andreae, M. O.: Analysis of aircraft and satellite measurements from the Intercontinental Chemical Transport Experiment (INTEX-B) to quantify long-range transport of East Asian sulfur to Canada, *Atmos. Chem. Phys.*, 8, 2999–3014, doi:10.5194/acp-8-2999-2008, 2008.
- van Vuuren, D. P., Edmonds, J., Kainuma, M., Riahi, K., Thomson, A., Hibbard, K., Hurtt, G. C., Kram, T., Krey, V., Lamarque, J. F., Masui, T., Meinshausen, M., Nakicenovic, N., Smith, S. J., and Rose, S. K.: The representative concentration pathways: an overview, *Clim. Change*, 109, 5–31, doi:10.1007/s10584-011-0148-z, 2011.
- Wan, Z. M., Zhang, Y. L., Zhang, Q. C., and Li, Z. L.: Validation of the land-surface temperature products retrieved from Terra Moderate Resolution Imaging Spectroradiometer data, *Remote Sens. Environ.*, 83, 163–180, doi:10.1016/s0034-4257(02)00093-7, 2002.
- Wang, Q., Jacob, D. J., Fisher, J. A., Mao, J., Leibensperger, E. M., Carouge, C. C., Le Sager, P., Kondo, Y., Jimenez, J. L., Cubison, M. J., and Doherty, S. J.: Sources of carbonaceous aerosols and deposited black carbon in the Arctic in winter-spring: implications for radiative forcing, *Atmos. Chem. Phys.*, 11, 12453–12473, doi:10.5194/acp-11-12453-2011, 2011.
- Westerling, A. L., Hidalgo, H. G., Cayan, D. R., and Swetnam, T. W.: Warming and earlier spring increase western US forest wildfire activity, *Science*, 313, 940–943, doi:10.1126/science.1128834, 2006.
- Wild, O., Zhu, X., and Prather, M. J.: Fast-j: accurate simulation of in- and below-cloud photolysis in tropospheric chemical models, *J. Atmos. Chem.*, 37, 245–282, doi:10.1023/a:1006415919030, 2000.
- Yevich, R. and Logan, J. A.: An assessment of biofuel use and burning of agricultural waste in the developing world, *Glob. Biogeochem. Cycle*, 17, 1095, doi:10.1029/2002GB001952, 2003.

Beyond direct radiative forcing

C. L. Heald et al.

[Title Page](#)

[Abstract](#)

[Introduction](#)

[Conclusions](#)

[References](#)

[Tables](#)

[Figures](#)

◀

▶

[Back](#)

[Close](#)

[Full Screen / Esc](#)

[Printer-friendly Version](#)

[Interactive Discussion](#)



Yu, H., Kaufman, Y. J., Chin, M., Feingold, G., Remer, L. A., Anderson, T. L., Balkanski, Y., Bel-  
louin, N., Boucher, O., Christopher, S., DeCola, P., Kahn, R., Koch, D., Loeb, N., Reddy, M. S.,  
Schulz, M., Takemura, T., and Zhou, M.: A review of measurement-based assessments of the  
aerosol direct radiative effect and forcing, *Atmos. Chem. Phys.*, 6, 613–666, doi:10.5194/acp-  
6-613-2006, 2006.

Zender, C. S., Bian, H. S., and Newman, D.: Mineral Dust Entrainment and Deposition  
(DEAD) model: description and 1990s dust climatology, *J. Geophys. Res.-Atmos.*, 108, 4416,  
doi:10.1029/2002JD002775, 2003.

Zhang, L., Jacob, D. J., Knipping, E. M., Kumar, N., Munger, J. W., Carouge, C. C., van Donkelaar, A., Wang, Y. X., and Chen, D.: Nitrogen deposition to the United States: distribution,  
sources and processes, *Atmos. Chem. Phys.*, 12, 4539–4554, doi:10.5194/acp-12-4539-  
2012, 2012.

Zhang, L. M., Gong, S. L., Padro, J., and Barrie, L.: A size-segregated particle dry deposition  
scheme for an atmospheric aerosol module, *Atmos. Environ.*, 35, 549–560, 2001.

## Beyond direct radiative forcing

C. L. Heald et al.

[Title Page](#)

[Abstract](#)

[Introduction](#)

[Conclusions](#)

[References](#)

[Tables](#)

[Figures](#)

◀

▶

[Back](#)

[Close](#)

[Full Screen / Esc](#)

[Printer-friendly Version](#)

[Interactive Discussion](#)



**Beyond direct radiative forcing**

C. L. Heald et al.

**Table 1.** Annual global aerosol or aerosol precursor emissions used in GCRT.

	Total Emissions (2010)	Anthropogenic Emissions* and Percent of Total in Brackets (2010)	Total Emissions (2100)
SO <sub>x</sub> (TgSyr <sup>-1</sup> )	63.8	53.3 (83 %)	19.5
NO <sub>x</sub> (TgNyr <sup>-1</sup> )	49.4	31.8 (64 %)	28.0
NH <sub>3</sub> (TgNyr <sup>-1</sup> )	55.9	37.9 (68 %)	56.3
POA (TgCyr <sup>-1</sup> )	29.3	9.3 (32 %)	20.4
BC (TgCyr <sup>-1</sup> )	6.8	4.5 (66 %)	4.4
Sea Salt (Tgyr <sup>-1</sup> )	3544	–	3544
Dust (Tgyr <sup>-1</sup> )	1563	312 (20 %)	1563

\* Includes fossil fuel, biofuel, and agriculture (but not biomass burning)

[Title Page](#)[Abstract](#)[Introduction](#)[Conclusions](#)[References](#)[Tables](#)[Figures](#)[|◀](#)[▶|](#)[◀](#)[▶](#)[Back](#)[Close](#)[Full Screen / Esc](#)[Printer-friendly Version](#)[Interactive Discussion](#)

Beyond direct  
radiative forcing

C. L. Heald et al.

**Table 2.** GCRT speciated dry aerosol size and optical properties.

	Geometric radius ( $r_g$ ) ( $\mu\text{m}$ )	Geometric Stdev ( $\sigma_g$ , log ( $\mu\text{m}$ ))	Refractive Index (550 nm)	Density ( $\text{g cm}^{-3}$ )
Sulfate, Nitrate and Ammonium	0.070	1.6	1.53–0.006i	1.7
OA	0.064	1.6	1.53–0.006i	1.8
BC	0.020	1.6	1.95–0.79i	1.8
Sea Salt				
accumulation	0.085	1.5	1.50–0.00000001i	2.2
coarse	0.40	1.8	1.50–0.00000001i	2.2
Dust	7 bins: 0.015, 0.25, 0.40, 0.80, 1.5, 2.5, 4.0	2.2	1.56–0.0014i	2.5

[Title Page](#)[Abstract](#)[Introduction](#)[Conclusions](#)[References](#)[Tables](#)[Figures](#)[|◀](#)[▶|](#)[◀](#)[▶](#)[Back](#)[Close](#)[Full Screen / Esc](#)[Printer-friendly Version](#)[Interactive Discussion](#)

**Table 3.** Global annual mean aerosol budget and impacts simulated for 2010 using GCRT (comparisons with AEROCOM II means from Myhre et al., 2013 in round brackets; comparisons with AEROCOM I medians from Kinne et al., 2006 in square brackets). Note anthropogenic here does not include biomass burning.

	Total	Sulfate	Nitrate	Ammonium <sup>a</sup>	BC	OA <sup>b</sup>	Sea Salt	Dust
Burden [Tg]	1.27 [1.99]	0.26	0.35	0.10 [0.20]	2.01 [1.68]	3.94 [6.43]	22.9 [19.9]	
Anthropogenic Fraction	0.60	0.82	0.82	0.57	0.21	0.0	0.20	
Anthropogenic Burden [Tg]	0.76 (0.91 ± 0.24)	0.21 (0.29 ± 0.14)	0.29	0.057 (0.071 ± 0.036)	0.44 (0.33 ± 0.23)	0.0	4.57	
AOD, 550 nm	0.092	0.0154 [0.034]	0.0031	0.0041	0.0012 [0.004]	0.0147 [0.019]	0.032 [0.030]	0.021 [0.032]
Anthro AOD, 550 nm	0.023 (0.030 ± 0.01)	0.0092 (0.021 ± 0.009)	0.0025 (0.0056 ± 0.0027)	0.0034	0.0007 (0.0015 ± 0.0005)	0.0029 (0.0062 ± 0.0071)	0.0	0.004
MEE = AOD/burden [m <sup>2</sup> g <sup>-1</sup> ]	6.3 (12.7 ± 8.6) [8.5]	5.7 (9.8 ± 2.0)	5.9	5.9 (10.5 ± 3.9) [8.9]	3.8 (7.5 ± 6.5) [5.7]	4.1 [3.0]	0.47 [0.95]	
TOA DRE, clear-sky [W m <sup>-2</sup> ]	-2.75	-0.54	-0.095	-0.14	0.10	-0.61	-1.10	-0.37
SW	-3.01	-0.55	-0.097	-0.14	0.10	-0.63	-1.16	-0.53
LW	0.26	0.01	0.002	0.003	0.002	0.02	0.06	0.16
TOA DRE, all-sky [W m <sup>-2</sup> ]	-1.83	-0.35	-0.067	-0.095	0.14	-0.42	-0.77	-0.26
SW	-2.03	-0.36	-0.069	-0.097	0.14	-0.43	-0.81	-0.40
LW	0.19	0.007	0.002	0.002	0.001	0.01	0.04	0.14
TOA DRF, clear-sky [W m <sup>-2</sup> ]	-0.57 (-0.67 ± 0.18)	-0.29	-0.079	-0.11	0.06	-0.075	0.0	-0.074
TOA DRF, all-sky [W m <sup>-2</sup> ]	-0.36 (-0.32 <sup>c</sup> ± 0.15)	-0.20 (-0.32 ± 0.11)	-0.055 (-0.08 ± 0.04)	-0.076	0.078 (0.18 ± 0.07)	-0.055 (-0.09)	0.0	-0.053

<sup>a</sup> Contributions from ammonium are included in sulfate and nitrate in AeroCom II

<sup>b</sup> We sum POA and SOA mean model values from AeroCom II

<sup>c</sup> Taken from Fig. 7 of Myhre et al. (2013)

## Beyond direct radiative forcing

C. L. Heald et al.

[Title Page](#)

[Abstract](#)

[Introduction](#)

[Conclusions](#)

[References](#)

[Tables](#)

[Figures](#)

◀

▶

◀

▶

[Back](#)

[Close](#)

[Full Screen / Esc](#)

[Printer-friendly Version](#)

[Interactive Discussion](#)



**Beyond direct  
radiative forcing**

C. L. Heald et al.

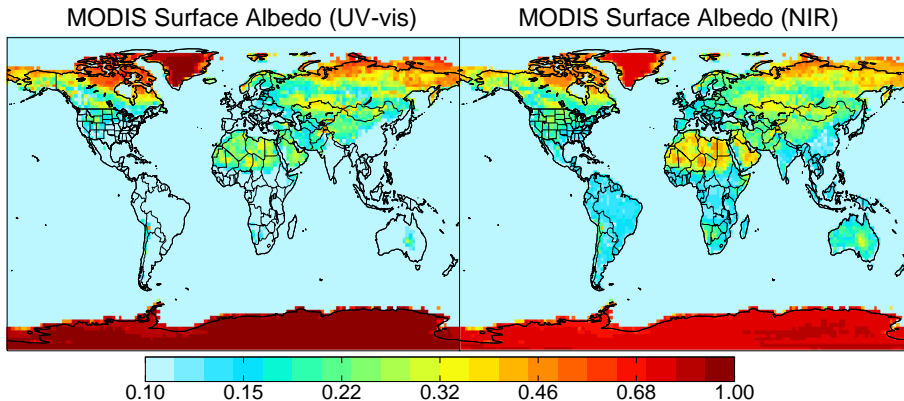


**Fig. 1.** Annual mean surface direct albedo in the UV-visible (left) and near-infrared (right) from MODIS 2002–2007 observations.

- [Title Page](#)
- [Abstract](#) [Introduction](#)
- [Conclusions](#) [References](#)
- [Tables](#) [Figures](#)
- [◀](#) [▶](#)
- [◀](#) [▶](#)
- [Back](#) [Close](#)
- [Full Screen / Esc](#)

- [Printer-friendly Version](#)
- [Interactive Discussion](#)



**Beyond direct  
radiative forcing**

C. L. Heald et al.

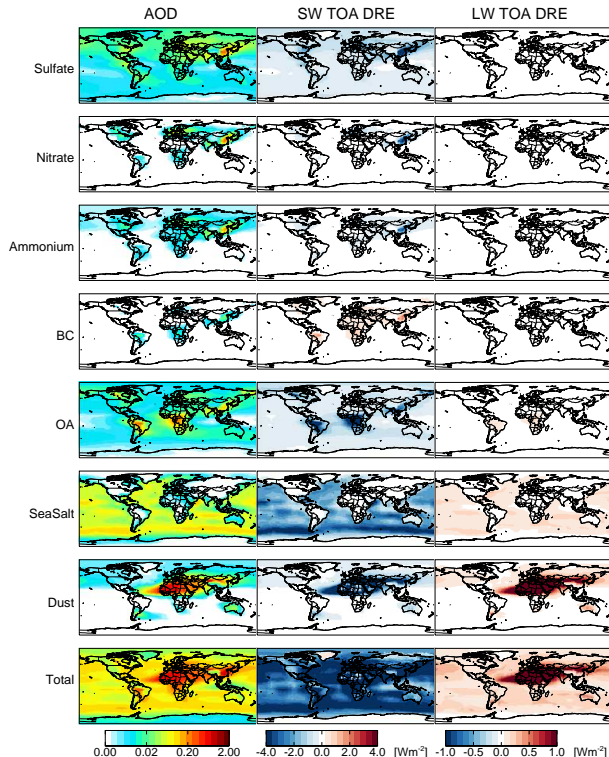


**Fig. 2.** Annual mean AOD (left), shortwave TOA clear-sky direct radiative effect (center) and longwave TOA clear-sky direct radiative effect (right) simulated by GCRT for 2010. Color bars are saturated at respective values.

[Title Page](#)[Abstract](#)[Introduction](#)[Conclusions](#)[References](#)[Tables](#)[Figures](#)[|◀](#)[▶|](#)[◀](#)[▶](#)[Back](#)[Close](#)[Full Screen / Esc](#)[Printer-friendly Version](#)[Interactive Discussion](#)

**Beyond direct radiative forcing**

C. L. Heald et al.

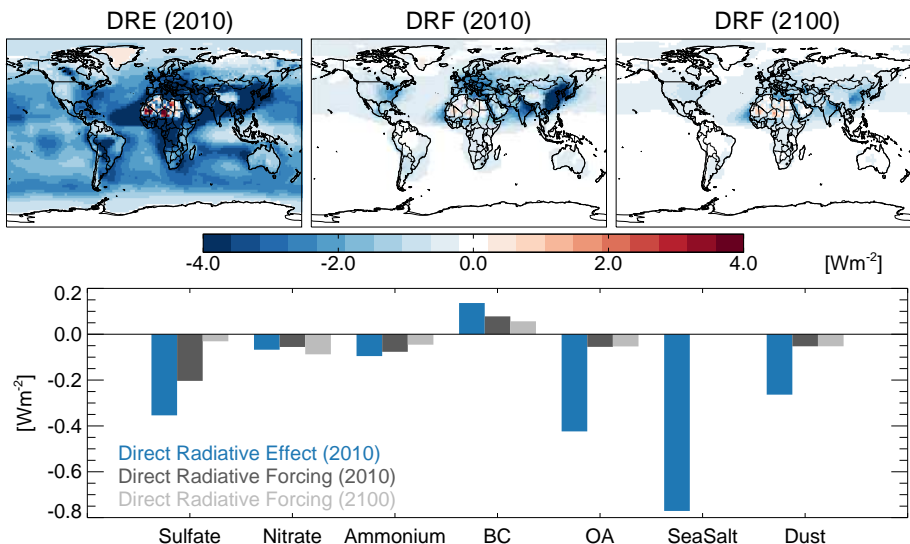


**Fig. 3.** Top: Global annual mean all-sky speciated aerosol TOA Direct Radiative Effect in 2010 (top left, blue), Direct Radiative Forcing for 2010 (top center, dark grey) and Direct Radiative Forcing for 2100 (top right, light grey). Mean values for 2010 are given in Table 3.

[Title Page](#)[Abstract](#)[Introduction](#)[Conclusions](#)[References](#)[Tables](#)[Figures](#)[|◀](#)[▶|](#)[◀](#)[▶](#)[Back](#)[Close](#)[Full Screen / Esc](#)[Printer-friendly Version](#)[Interactive Discussion](#)

**Beyond direct radiative forcing**

C. L. Heald et al.

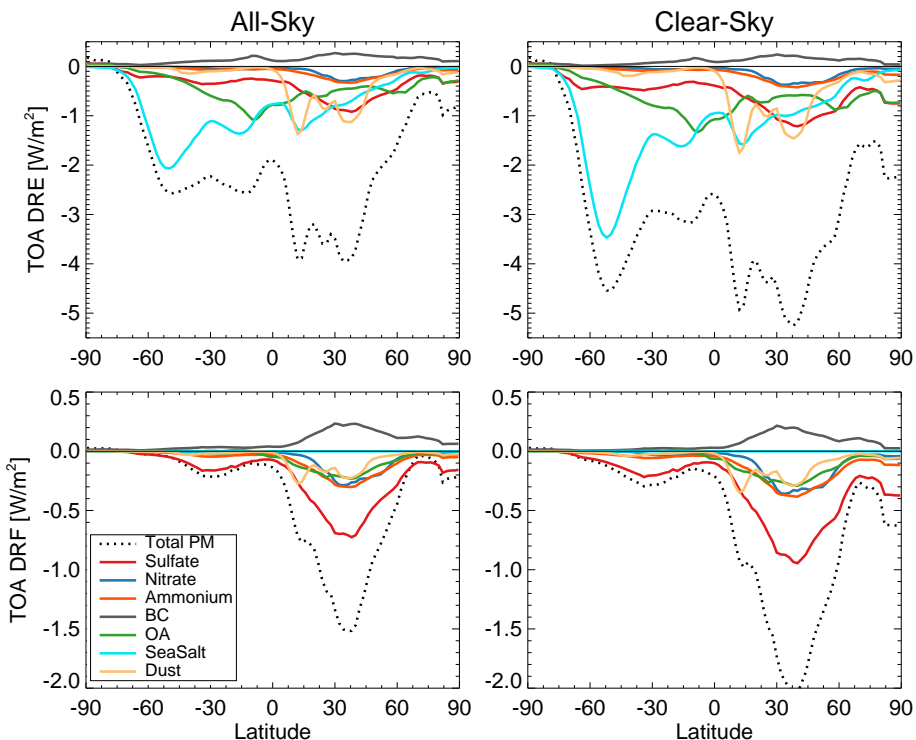


**Fig. 4.** Global zonal mean all-sky spiated aerosol TOA direct radiative effect (top) and direct radiative forcing (bottom) for all-sky (left) and clear-sky (right) simulated by GCRT for 2010.

<a href="#">Title Page</a>	<a href="#">Abstract</a>	<a href="#">Introduction</a>
<a href="#">Conclusions</a>	<a href="#">References</a>	
<a href="#">Tables</a>	<a href="#">Figures</a>	
<a href="#"></a>	<a href="#"></a>	
<a href="#">Back</a>	<a href="#">Close</a>	
<a href="#">Full Screen / Esc</a>		

[Printer-friendly Version](#)[Interactive Discussion](#)

## Beyond direct radiative forcing

C. L. Heald et al.

[Title Page](#)

[Abstract](#)

[Introduction](#)

[Conclusions](#)

[References](#)

[Tables](#)

[Figures](#)

◀

▶

◀

▶

[Back](#)

[Close](#)

[Full Screen / Esc](#)

[Printer-friendly Version](#)

[Interactive Discussion](#)

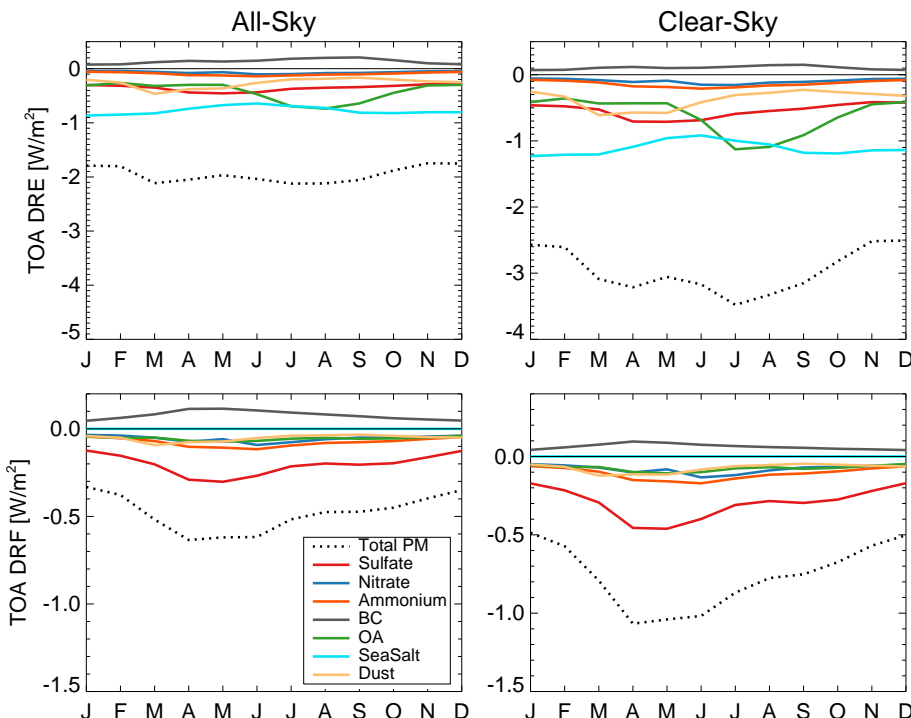


**Fig. 5.** Global seasonal mean speciated aerosol TOA direct radiative effect (top) and direct radiative forcing (bottom) for all-sky (left) and clear-sky (right) simulated by GCRT for 2010.

## Beyond direct radiative forcing

C. L. Heald et al.

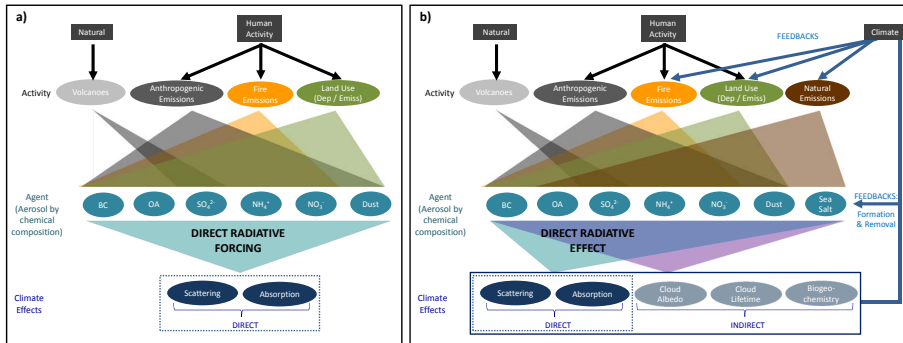


**Fig. 6.** Illustration highlighting the difference between the estimate of **(a)** Direct Radiative Forcing and **(b)** Direct Radiative Effect (right). DRF is the perturbation (since pre-industrial) associated with human activity and natural forcing (i.e. volcanoes). DRE characterizes the instantaneous impact of all aerosols on radiation (including any feedbacks and natural processes).

<a href="#">Title Page</a>	<a href="#">Abstract</a>	<a href="#">Introduction</a>
<a href="#">Conclusions</a>	<a href="#">References</a>	
<a href="#">Tables</a>	<a href="#">Figures</a>	
<a href="#">◀</a>	<a href="#">▶</a>	
<a href="#">◀</a>	<a href="#">▶</a>	
<a href="#">Back</a>	<a href="#">Close</a>	
<a href="#">Full Screen / Esc</a>		

<a href="#">Printer-friendly Version</a>
<a href="#">Interactive Discussion</a>

